JOURNAL OF MATERIALS SCIENCE **38** (2003) 2825–2833

The ballistic impact characteristics of Kevlar® woven fabrics impregnated with a colloidal shear thickening fluid

YOUNG S. LEE
Department of Chemical Engineering and Center for Composite Materials, University of Delaware, Newark, DE 19716, USA

E. D. WETZEL
Army Research Laboratory, Aberdeen Proving Ground, MD 21005, USA

N. J. WAGNER*
Department of Chemical Engineering and Center for Composite Materials, University of Delaware, Newark, DE 19716, USA
E-mail: wagner@che.udel.edu

This study reports the ballistic penetration performance of a composite material composed of woven Kevlar® fabric impregnated with a colloidal shear thickening fluid (silica particles (450 nm) dispersed in ethylene glycol). The impregnated Kevlar fabric yields a flexible, yet penetration resistant composite material. Fragment simulation projectile (FSP) ballistic penetration measurements at ~244 m/s have been performed to demonstrate the efficacy of the novel composite material. The results demonstrate a significant enhancement in ballistic penetration resistance due to the addition of shear thickening fluid to the fabric, without any loss in material flexibility. Furthermore, under these ballistic test conditions, the impregnated fabric targets perform equivalently to neat fabric targets of equal areal density, while offering significantly less thickness and more material flexibility. The enhancement in ballistic performance is shown to be associated with the shear thickening response, and possible mechanisms of fabric-fluid interaction during ballistic impact are identified.

1. Introduction

The primary objective of body armor research is to develop a low cost, lightweight, wearable garment system with ballistic impact resistance [1]. Body armor standards require that a projectile should be stopped under ballistic impact, and that the penetration depth into a clay witness backing the armor should not exceed 1.73 inches [2]. If penetration depth exceeds this value, a wearer can incur serious blunt trauma [3]. Aramid (Kevlar®) and ultra high molecular weight polyethylene (Spectra®) have been introduced as base materials for ballistic protection. These high performance fibers are characterized by low density, high strength, and high energy absorption [4]. However, to meet the protection requirements for typical ballistic threats, approximately 20–50 layers of fabric are required. The resulting bulk and stiffness of the armor limits its comfort, and has restricted its application primarily to torso protection.

Shear thickening is a non-Newtonian flow behavior often observed in concentrated colloidal dispersions characterized by significant, sometimes discontinuous increase in viscosity with increasing shear stress [5–7]. It has been demonstrated that reversible shear thickening in concentrated colloidal suspensions is due to the formation of jamming clusters resulting from hydrodynamic lubrication forces between particles, often denoted by the term "hydroclusters" [8–11]. The mechanism of shear thickening has been studied extensively by rheo-optical experiments [12, 13], neutron scattering [14–18] and stress-jump rheological measurements [19]. The onset of shear thickening in steady shear can now be quantitatively predicted [17, 20] for colloidal suspensions of hard-spheres and electrostatically stabilized dispersions.

This shear thickening phenomenon can damage processing equipment and induce dramatic changes in suspension microstructure, such as particle aggregation, which results in poor fluid and coating qualities. The highly nonlinear behavior can provide a self-limiting maximum rate of flow that can be exploited in the design of damping and control devices [21, 22]. Here, we propose to utilize this shear thickening phenomena to enhance the ballistic protection afforded by fabric-based, flexible body armor.

*Author to whom all correspondence should be addressed.

A previous study investigated a related, but distinct effect to improve the performance of Kelvar woven fabrics. Dischler *et al*. [23] used fibers coated with a dry powder that exhibits dilatant properties. In their work, the fibers demonstrated an improved ability to distribute energy during ballistic impact due to the enhanced inter-fiber friction.

The objective of this study is to investigate the ballistic properties of woven Kevlar fabrics impregnated with fluids that exhibit the shear thickening effect. At low strain rates, associated with normal motion of the wearer, the fluid will offer little impediment to fabric flexure and deformation. However, at the high strain rates associated with a ballistic impact event, the fluid will thicken and in doing so, enhance the ballistic protection of the fabric. The results of this study confirm these hypotheses, and demonstrate that the novel composite material could provide a more flexible, and less bulky, alternative to neat Kevlar fabrics.

2. Experimental

2.1. Materials

2.1.1. Shear thickening fluid

The colloidal silica used to produce the shear thickening fluids (STFs) for this investigation (Nissan Chemicals (MP4540)) is provided as an aqueous suspension at a particle concentration of about 40 wt%. The particle size was characterized with dynamic light scattering and transmission electron microscopy (TEM). Fig. 1 shows the TEM micrographs of a dried sample of the dispersion. The particles are bimodal in size, with a minor fraction of smaller particles. The average particle diameter was determined to be 446 nm by dynamic light scattering. The density of the silica particles was calculated from density measurements (DMA 48 density meter (Anton Paar)) conducted on dilute samples of the dispersion. The weight fraction of silica in each solution was measured by drying in a convection oven at 180°C for 5 h and weighing the residual dry silica. From the mass fraction, solvent density and the corresponding measured solution density, the density of the silica particles in solution was estimated to be 1.78 g/cc.

As a means of preparing a stable, shear thickening concentrated dispersion, the aqueous medium was replaced with ethylene glycol. Ethylene glycol was chosen as a solvent due to its low volatility and thermal stability. Additionally, the index of refraction of ethylene glycol is close to that of the silica particles, providing enhanced colloidal stability. Three hours of centrifugation at 3,900 rpm using a table top centrifuge (IEC clinical centrifuge) was performed to separate the silica particles from the aqueous-based supernatant. The silica sediment was then crushed using a spatula and resuspended in ethylene glycol using a vortex mixer. This process was repeated 4 times in order to minimize the amount of residual aqueous supernatant present within the samples. The final weight fraction of particles in this stock solution was determined by using a moisture analyzer (Mettler Toledo, HR73).

Rheological measurements were performed primarily with a stress-controlled rheometer (SR-500, Rheometrics) at 25°C with cone-plate geometry having a cone angle of 0.1 radian and a diameter of 25 mm. Complementary measurements were performed on a Rheometrics ARES controlled strain rheometer. To minimize the effects of solvent evaporation during testing, a solvent trap was used during all rheometer measurements. To remove sample loading effects, a preshear of 1 s^{-1} was applied for 60 s prior to further measurement. All measurements presented here were reproducible.

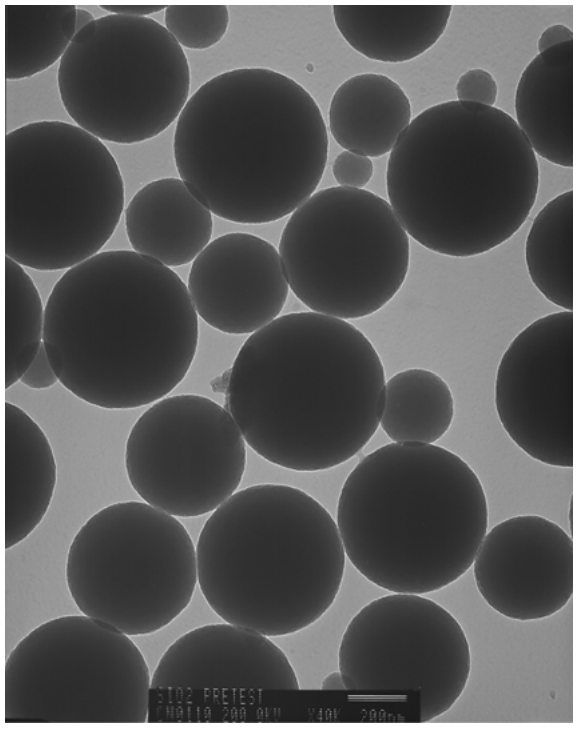

Figure 1 Transmission electron microscopy of colloidal silica obtained from Nissan Chemicals (MP4540) at a magnification of 40,000.

2.1.2. Kevlar fabric

The Kevlar fabric used in all composite target constructions was plain-woven Hexcel Aramid (poly-paraphenylene terephthalamide), high performance fabric Style 706 (Kevlar KM-2, 600 denier) with an areal density of 180 g/m^2.

2.2. Target preparation

Ethylene glycol (surface tension = 47.7 dyne/cm) was observed to wet the Kevlar fabric. To facilitate impregnation of the STF into the Kevlar fabric, an equal volume of ethanol surface tension (22.0 dyne/cm) was added to the original ethylene glycol based STF. This diluted STF was observed to spontaneously impregnate the fabric. Following impregnation, the composite fabric was heated at 80°C for 20 min in a convection oven to remove the ethanol from the sample. The final composition of the impregnated STF is 57 vol% silica in ethylene glycol.

Fig. 2 shows an SEM image of one such STF-impregnated fabric. The ethylene glycol was removed prior to imaging by drying the sample at 200°C for 24 h, leaving only the silica particles and Kevlar fabric. The image shows silica particles dispersed within the yarn,

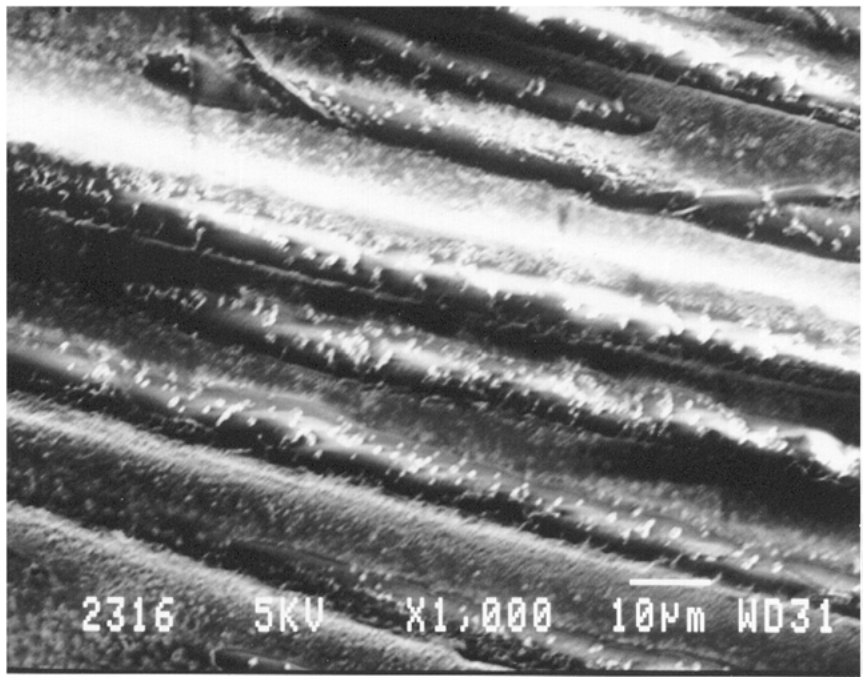

Figure 2 Scanning electron microscopy of Kevlar weave impregnated with the STF.

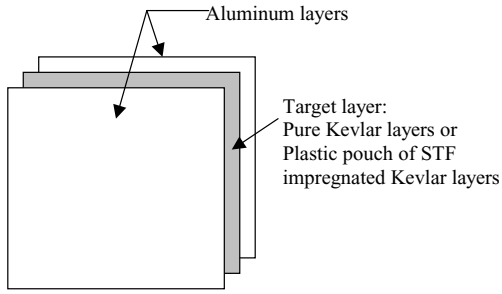

Figure 3 Schematic diagram of target structure.

demonstrating that the original STF was fully impregnated between the individual Kevlar fibers within each yarn.

In addition to the STF-impregnated fabric, samples were made of fabric impregnated with neat ethylene glycol. The ethylene glycol-impregnated fabric was made using the same ethanol dilution and evaporation method used for the STF-impregnated targets.

Fig. 3 is a schematic diagram of a ballistic target. Two pieces of 5.08 cm × 5.08 cm aluminum foil (50 μm thickness) were used to encapsulate the targets. The Kevlar layers were cut to 4.76 cm × 4.76 cm, impregnated with varying amounts of STF per layer (2, 4, and 8 ml) as indicated, and then assembled into the targets by stacking them to the desired target configuration. To prevent leakage of STF out of the target assembly and because Kevlar® is known be sensitive to moisture, heat-sealed polyethylene film (Ziplock bags sealed using a ULINE KF-200HC heat sealer) was used to encapsulate the targets. Neither the aluminum foil nor the polyethylene packaging provided any measurable ballistic resistance.

These targets were mounted onto a single ply of unimpregnated Kevlar, glued to a 5.08 cm diameter copper hoop (0.635 cm wire diameter) using Liquid Nails adhesive (ICI), in order to help support the target during testing. In all cases this mounted Kevlar layer was immediately adjacent to the ballistic target, with the copper hoop resting inside of the target mounting frame. All subsequent descriptions of ballistic targets will list only the Kevlar layers within the aluminum foil layers, and do not include this individual backing Kevlar layer.

2.3. Ballistic tests

The ballistic tests were performed using a smooth bore helium gas gun (Army Research Laboratory, MD). All tests were performed at room temperature. The gun was sighted on the target center and the impact velocity was adjusted to approximately 244 m/s (800 fps). The exact impact velocity of each projectile was measured with a chronograph immediately before impacting the target. The projectile is a NATO standard fragment simulation projectile (FSP), consisting of a chisel-pointed metal cylinder of 1.1 grams (17 grains) and 0.56 cm diameter (22 caliber). A 10.16 cm × 10.16 cm × 2.54 cm thick aluminum block was cut with a recessed square hole to accept the 5.08 cm square target package (Fig. 4). The target was held in place using light pressure from spring clips located along its edge. The mounting block was then clamped onto a steel frame in line with the gas gun barrel.

A clay witness was used to measure the depth of indentation [2] (Fig. 4). Modeling clay (Van Aken International) was packed into a 15.24 cm × 8.89 cm × 8.89 cm wooden mold, compressed with a mallet, and cut into four 7.62 cm × 4.45 cm square pieces. This process minimizes air bubbles or poor compaction in the clay witness. The molded clay block was held onto the back of the target using a strip of adhesive tape.

In order to normalize results with respect to variations in impact velocities, ballistic test results are also presented in terms of dissipated projectile kinetic

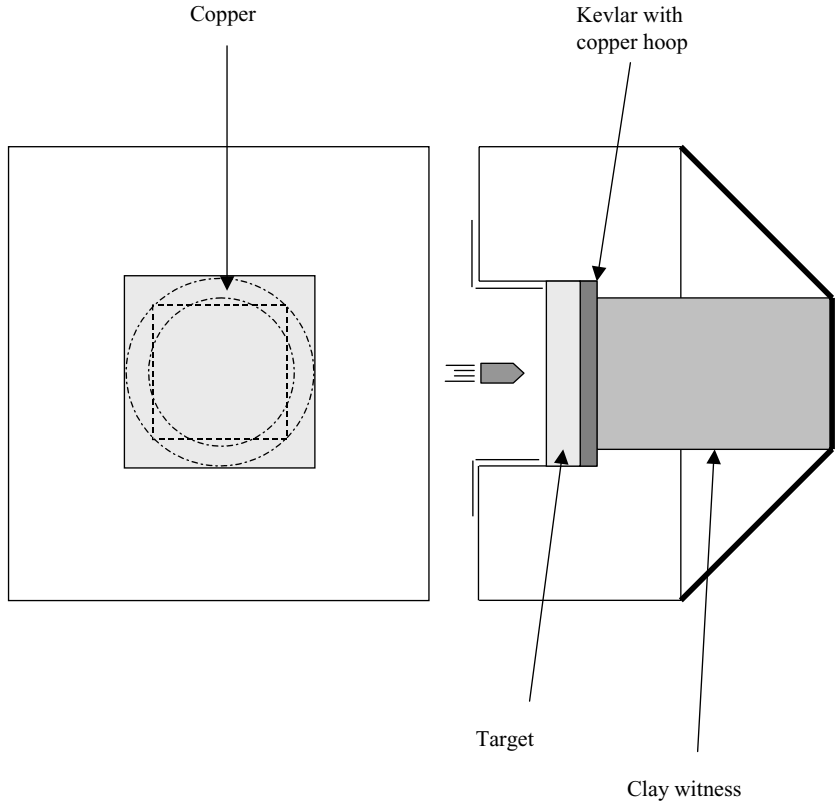

Figure 4 Schematic diagram of ballistic experimental setup.

energy

$$E = \frac{1}{2} m_{\mathrm{p}} \left(V_{\mathrm{i}}^2 - V_{\mathrm{r}}^2 \right) \tag{1}$$

where E is the dissipated energy (J), m_{p} is the projectile mass (kg), V_{i} is the initial projectile velocity (m/s), and V_{r} is the residual velocity of the projectile after penetrating the target (m/s). In order to relate depth of penetration to residual projectile velocity, a series of experiments were performed using an empty target frame and clay witness. Fig. 5 shows the resulting penetration depth as a function of projectile velocity, which is closely modeled by the linear relationship

$$V_{\mathrm{r}} = 38.9 + 3720\, L \tag{2}$$

where L (m) is the penetration depth into the clay witness. Equations 1 and 2 are used throughout this paper to relate depth of penetration to residual projectile kinetic energy. The energy dissipated by the target is normalized by the initial kinetic energy of the projectile to obtain the fractional dissipation.

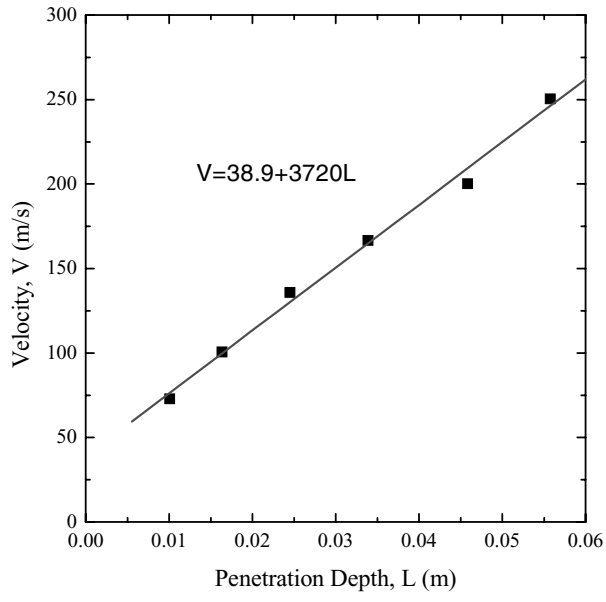

Figure 5 Relationship between penetration depth of projectile in clay witness and velocity of projectile with empty target frame.

2.4. Flexibility and thickness tests

Two-dimensional drape tests were performed to measure the flexibility of the targets, as shown in Fig. 6.

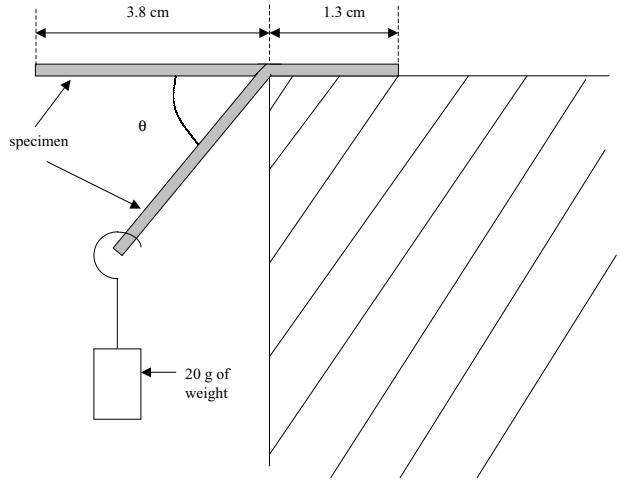

Figure 6 Test set up for flexibility measurement of sample.

In all cases a 20 g weight was used, and encapsulated ballistic targets were used as the test specimens. Bending angle is reported as a measure of target flexibility, with larger angles indicating greater flexibility. Target thickness at the center of the targets was also measured with a micrometer.

3. Results

3.1. Rheological properties of shear thickening suspension

Fig. 7 shows the steady shear viscosity as a function of the steady shear rate for the ethylene glycol based silica suspension at volume fractions of $\phi = 0.57$ and 0.62. Note that the data are collected on a controlled stress rheometer where an applied shear stress is controlled and the corresponding shear rates measured. However, the data has been plotted against the measured shear rate rather than the applied stress, as is more traditional. The use of controlled stress enables probing the regime of extreme shear thickening observed at high shear rates, which is not possible in a controlled rate device due to the nature of the material's response. Both shear thinning and shear thickening behavior are observed. At these high particle loadings, the silica suspensions are glassy at rest and yield at low shear rates. This manifests in Fig. 7 as strong shear thinning $\eta(\dot{\gamma}) \propto \dot{\gamma}^{-1}$, which is a signature of a yield stress [24]. With increasing shear rate the viscosity begins to plateau, followed by a transition to shear thickening behavior at high shear rates. The shear thickening transition was observed to occur at shear rate of 10 s^{-1} for the concentrated dispersion having a particle volume fraction of $\phi = 0.62$ and 300 s^{-1} for the fluid with a particle volume fraction of $\phi = 0.57$. At high shear rates in the shear thickening region, the high volume fraction ($\phi = 0.62$) dispersion exhibits a greater increase in viscosity. Transducer limitations and sample adhesive failure to the tooling prevented exploration of higher shear stresses. However, careful analysis of the slip in these materials [20, 25] demonstrates that the sample solidifies in the shear thickened regime, such that the reported viscosities after the onset of shear thickening are more representative of the suspension slipping against the tooling. Note also that the shear thickening transition is reversible, i.e., this liquid-to-solid transition induced by flow is not associated with particle aggregation, nor does it result in any irreversible change in the dispersion. This effect is shown in Fig. 7, as the data plotted corresponds to both ascending and descending shear stresses without hysteresis.

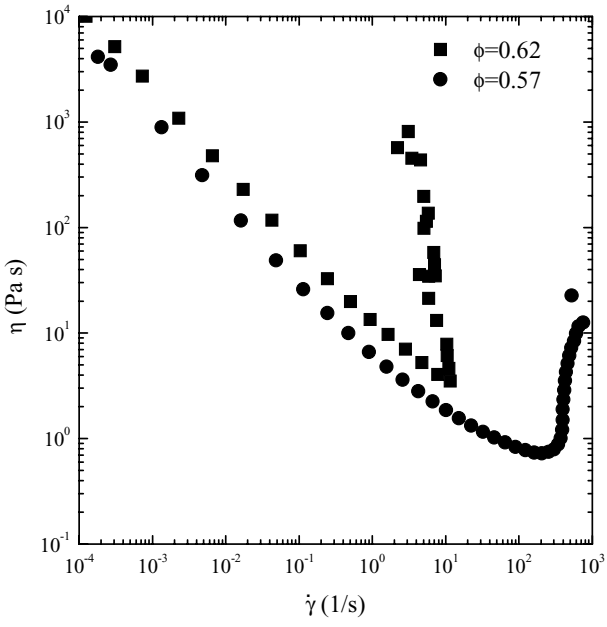

Figure 7 Shear thickening behavior of 57 and 62 volume % colloidal silica dispersed in ethylene glycol for steady shear flow.

The shear thickening transition in colloidal dispersions is believed to result from a microstructural change where the hydrodynamic forces overcome interparticle forces to create particle clusters [26]. These cluster formations, referred to as "hydroclusters," increase the hydrodynamic stress in the suspension, thus marking the onset of shear thickening. The hydroclustered state, however, does not lead to permanent or irreversible particle aggregation. Additional rheological studies have shown that the timescales for this transition are on the order of millisecond or less [15, 20, 25].

The characteristic shear rate for the ballistic testing performed here is estimated to be on the order of 45,000 1/s ($\dot{\gamma} = v_x/y = 24400/0.56$), based on a projectile velocity of 800 fps (244 m/s) and a projectile diameter of 22 caliber (0.56 cm). This shear rate greatly exceeds the rate required for the onset of shear thickening in this fluid (about 300 1/s for the silica suspension with $\phi = 0.57$). Thus we expect the shear rates during the ballistic tests to be sufficient to transition the dispersion to its shear thickened state.

3.2. Ballistic test results

The ballistic test results of a series of targets composed of 4 layers of Kevlar and 8 mL of STF with different configurations (targets A to F in Fig. 8) are shown in Figs 9–11 and summarized in Table I. The projectile has been stopped in all targets. Fig. 9 shows the energy dissipation for these targets, with the fully impregnated targets (E, F) showing significantly less penetration depth than the unimpregnated targets (A, B, C, D). The clay witness penetration profiles (Fig. 10) also show a marked difference in shape, as the unimpregnated targets show sharp, deep penetration profiles, while the impregnated samples show a blunt, shallow impregnation. These results clearly show that impregnating the STF into the fabric is critical to achieving an enhancement in the fabric ballistic properties.

Fig. 11 shows the front Kevlar layers for targets D (unimpregnated) and F (impregnated). The unimpregnated target shows that the Kevlar yarns that were directly impacted by the projectile pullout significantly from the weave, producing the well-documented cross pattern in the fabric. Note that the Kevlar layers exhibit little actual fiber breakage, although some fiber stretching near the impact point may have occurred. In contrast, the first layer of Kevlar in the impregnated target shows extensive fiber breakage near the projectile

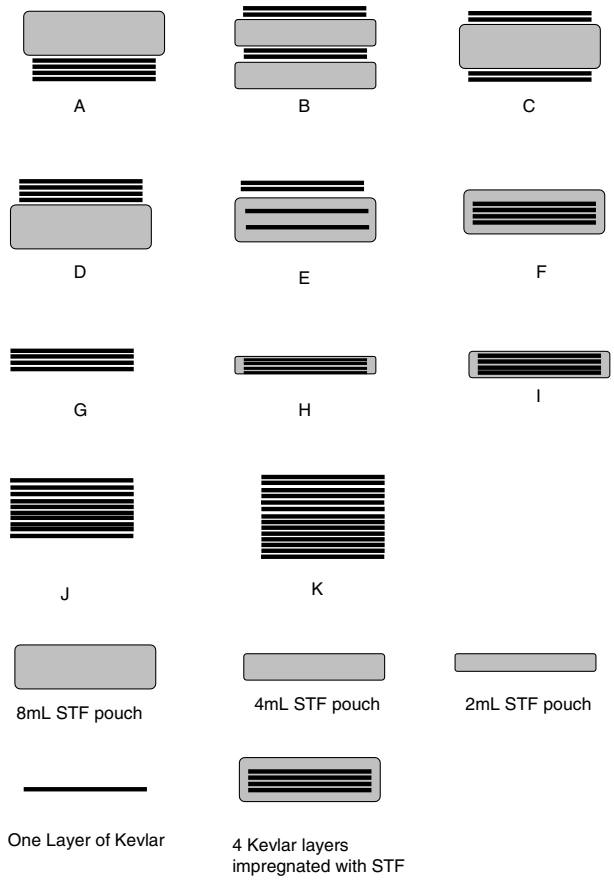

Figure 8 Schematic of the targets studied.

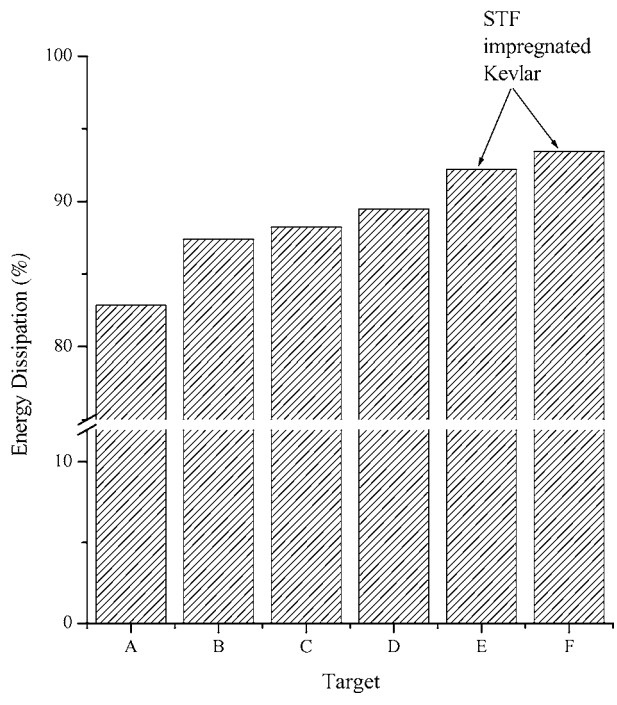

Figure 9 Result of energy dissipation with different target design.

contact point, and only very little yarn pullout or wrinkling in the surrounding fabric. Some fiber stretching may have occurred at the impact point. Note that yarn pullout is evident only for the yarns directly impacted by the projectile, with the total pullout distance significantly less than that observed for the neat Kevlar target.

Having demonstrated that fabric impregnation is essential to realizing enhanced performance, further targets were constructed to establish the scaling of energy absorption with the relative amount of STF and Kevlar in the target. Table II and Fig. 12 show the energy dissipated by targets consisting of 4 impregnated layers of fabric, as a function of the volume of STF. As shown in this figure, the energy absorption by the target increases continuously with the total volume of STF in the target.

To demonstrate that the enhanced ballistic performance of the impregnated fabrics is not simply a consequence of increased target mass or solvent effects on the Kevlar weave, tests were performed using Kevlar that was impregnated with pure ethylene glycol. As shown in Fig. 12, samples of ethylene glycol-impregnated Kevlar show relatively poor ballistic performance compared with STF-impregnated Kevlar with equal impregnated fluid volume. In this graph, the dotted line shows the amount of energy dissipated by 4 layers of pure Kevlar (target G). The results show that the addition of ethylene glycol does not improve the impact energy absorption capacity of Kevlar fabric. In fact, at high loadings (8 ml ethylene glycol) the performance is even worse than neat Kevlar, despite the increased target mass. This decrease in performance may be due to lubrication effects, as the solvent (which is Newtonian at these shear rates, unlike the shear thickening fluid) may reduce the friction between fibers in the fabric during yarn pullout.

A direct comparison between the ballistic protection performance of targets consisting of pure Kevlar fabric

TABLE I Test results of samples with 4 layers of Kevlar and 8 ml of shear thickening fluid with different configurations but equal target weights

Target	Description	Sample weight (g)	Impact velocity (m/s)	Penetration depth (cm)	Dissipated energy (Joule)
A	8 ml STF-K-K-K-K	13.9	247	1.72	27.8
B	K-K-4 ml STF-K-K-4 ml STF	13.9	249	1.36	29.8
C	K-K-8 ml STF-K-K	13.9	244	1.22	28.9
D	K-K-K-K-8 ml STF	13.9	253	1.19	31.5
E	K-K-8 ml STF impregnated in 2 layers of Kevlar	13.9	242	0.787	29.7
F	8 ml STF impregnated in 4 layers of Kevlar	13.9	253	0.673	32.9

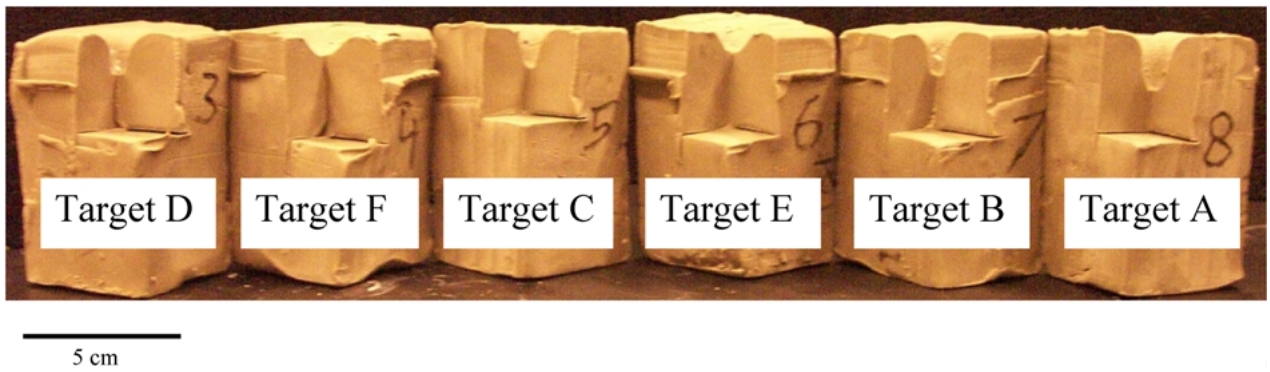

Figure 10 Penetration depth of the projectile in the clay witness for the STF umimpreganted (A–D) and impregnated (E, F) Kevlar samples.

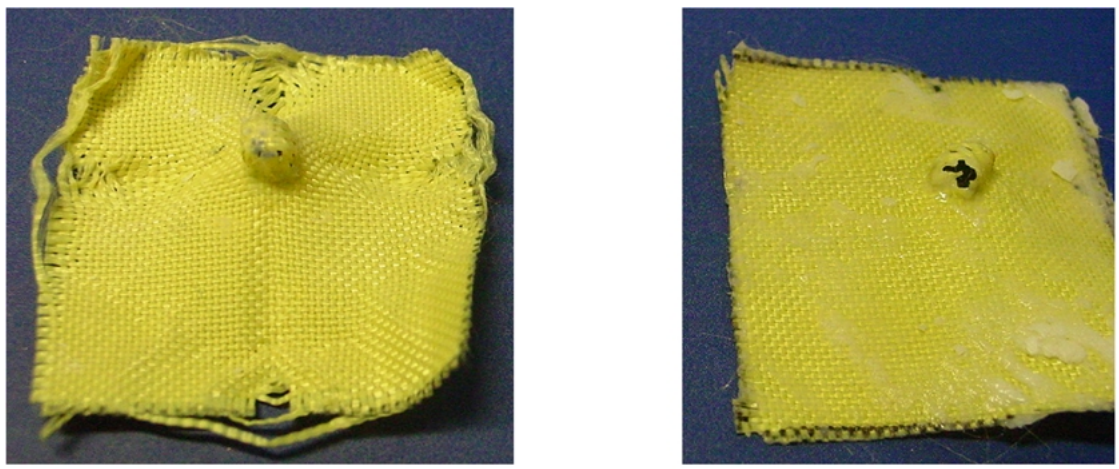

Figure 11 Comparison of front Kevlar layers for (a) unimpregnated (target D) and (b) impregnated (target F) target after ballistic test.

and STF-impregnated Kevlar fabric with nearly equal total weight has been made in Table III and Fig. 13. As shown in Fig. 13, the composite, impregnated targets have the same ballistic resistance as targets of equal weight of pure Kevlar. However, the number of layers of Kevlar in the impregnated samples is significantly fewer than the number of Kevlar layers in the neat Kevlar targets.

TABLE II Effect of amount of shear thickening fluid impregnated in 4 layers of Kevlar on ballistic performance

Target	Description	Sample weight (g)	Impact velocity (m/s)	Penetration depth (cm)	Dissipated energy (Joule)
G	4 layers of Kevlar	1.9	244	2.12	25.1
H	2 ml STF impregnated in 4 layers of Kevlar	4.8	243	1.23	28.6
I	4 ml STF impregnated in 4 layers of Kevlar	7.9	244	0.886	29.9
F	8 ml STF impregnated in 4 layers of Kevlar	13.9	253	0.673	32.9

3.3. Flexibility and thickness test results

The test results for the flexibility of 4 layers of Kevlar, 10 layers of Kevlar and 4 layers of Kevlar impregnated with 2 ml STF are presented in Table IV. The weight and ballistic performance of the 4-layer STF-impregnated Kevlar is nearly the same as that of the 10-layer unimpregnated Kevlar. However, the 4-layer STF-impregnated Kevlar is more flexible (bending angle = 51°) than the 10-layer unimpregnated Kevlar (bending angle = 13°) with same overall weight. In fact, there is no difference in flexibility between the

TABLE III Comparison of ballistic performance for shear thickening fluid impregnated in 4 layers of Kevlar and pure Kevlar with varying target weights

Target	Description	Sample weight (g)	Impact velocity (m/s)	Penetration depth (cm)	Dissipated energy (Joule)
J	10 layers of Kevlar	4.7	247	1.55	28.6
H	2 ml STF impregnated in 4 layers of Kevlar	4.8	243	1.23	28.6
K	14 layers of Kevlar	6.6	251	1.05	31.2
I	4 ml STF impregnated in 4 layers of Kevlar	7.9	244	0.886	29.9
F	8 ml STF impregnated in 4 layers of Kevlar	13.9	253	0.673	32.9

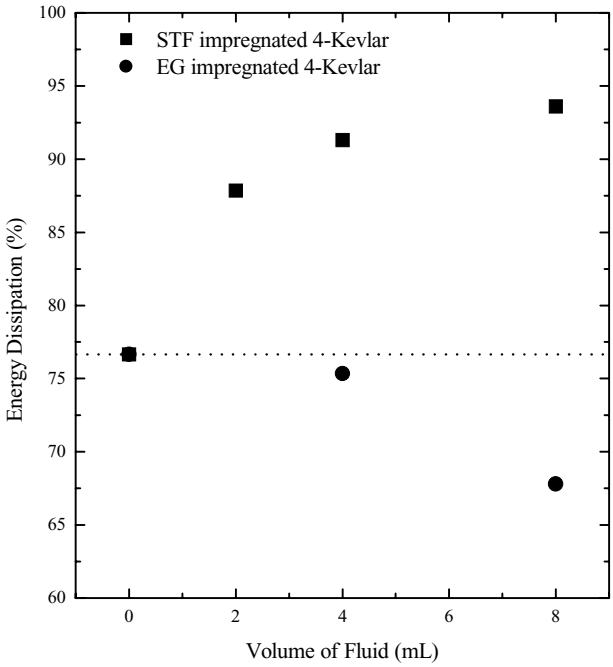

Figure 12 Dissipated energy as a function of volume of the fluid for the STF and ethylene glycol impregnated Kevlars. All targets have 4 layers of Kevlar.

4-layer Kevlar samples with and without impregnated STF (bending angle = 50°), indicating that the addition of STF causes no change in the flexibility of Kevlar fabrics at low rates of deformation, in contrast to the behavior at much higher deformation rates characteristic of the ballistic tests.

The target thicknesses are also given in Table IV. Note that the 10-layer neat Kevlar thickness (3.0 mm) is much greater than the 4-layer STF-impregnated Kevlar thickness (1.5 mm), which is only slightly thicker than the 4-layer neat Kevlar target (1.4 mm). Therefore

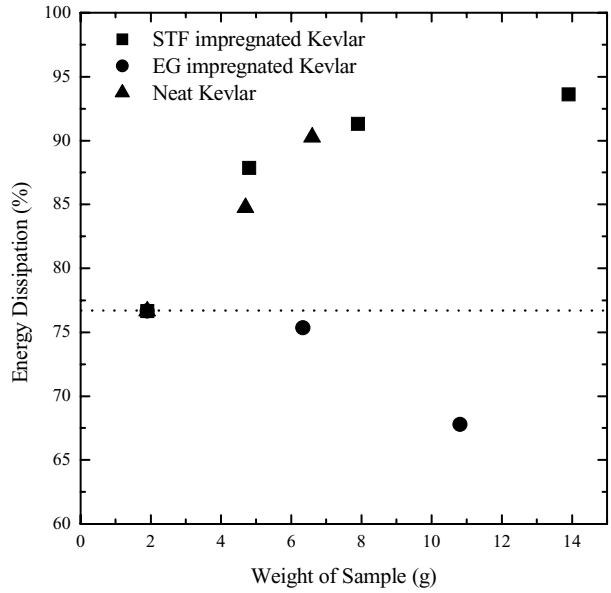

Figure 13 Dissipated energy as a function of weight of sample for the STF, ethylene glycol impregnated Kevlars and pure Kevlar.

the STF-impregnated target exhibits significantly less thickness, or bulk, than the neat Kevlar target of equivalent weight and ballistic performance.

4. Discussion

The results of Section 3.2 clearly demonstrate that, under our test conditions, impregnating neat Kevlar fabric with STF enhances the ballistic properties of the fabric. More precisely, the addition of STF to the fabric increases the amount of projectile energy that is absorbed by the target. A number of possible mechanisms could explain this behavior. Fig. 11 shows that the impregnated fabric exhibits significantly less pullout that the unimpregnated fabric, both in terms of the number of yarns pulled and the pullout distance per yarn. The impregnated target, unlike the neat fabric, also exhibits significant fiber fracture at the impact point. Another important difference is that all four layers of fabric in target D (not shown) exhibited extensive pullout, comparable to that of the first layer of fabric. In contrast, the three backing layers of target F (not shown) exhibited little or no pullout, and no fiber fracture. Therefore, most of the energy absorption in the impregnated target was likely provided by the first layer of Kevlar, although the backing layers may still have provided a critical secondary role during the impact event.

These results suggest that the STF constrains the Kevlar yarns as they are pulled through the fabric. The increase in energy dissipation in the impregnated target

TABLE IV Flexibility and thickness for pure Kevlar and STF impregnated Kevlar

Target	Description	Sample weight (g)	Penetration depth (cm)	Dissipated energy (Joule)	Bending angle, θ (°)	Sample thickness (mm)
G	4 layers of Kevlar	1.9	2.12	25.1	50	1.4
J	10 layers of Kevlar	4.7	1.55	28.6	13	3.0
H	2 ml STF impregnated in 4 layers of Kevlar	4.8	1.23	28.6	51	1.5

could be due in part to an increase in force required to pullout each yarn from the fabric, so that less total pullout is required to absorb the projectile energy. An alternative explanation is that the increased pullout resistance increases the loads on the yarns during impact, which then absorb additional energy through fiber deformation and fracture. To address these issues, we are performing additional ballistic tests at higher velocities, and performing quasistatic yarn pullout tests [3, 27] with and without STF.

It is important to point out that the targets used in these experiments are significantly smaller in area than the fabric used in full body armor. Therefore it is possible that the ballistic defeat mechanisms in our targets are somewhat different from those of larger targets, especially with respect to the total extent of pullout. However, these experiments do demonstrate that the addition of STF provides a means of tailoring the mechanisms of pullout and failure in Kevlar fabric. We are performing experiments on larger STF-impregnated Kevlar targets, with varying amounts of STF and patterns of STF impregnation, in order to identify the most efficient strategy for utilizing the STF-Kevlar composite's unique properties.

5. Conclusions and future work

This study demonstrates that the ballistic penetration resistance of Kevlar fabric is enhanced by impregnation of the fabric with a colloidal shear thickening fluid. Impregnated STF-fabric composites are shown to provide superior ballistic protection as compared with simple stacks of neat fabric and STF. Comparisons with fabrics impregnated with non-shear thickening fluids show that the shear thickening effect is critical to achieving enhanced performance. Energy absorption by the STF-fabric composite is found to be proportional to the volume of STF. Compared with neat Kevlar fabrics of equivalent weight, the STF-impregnated Kevlar fabric provides nearly the same ballistic protection, yet is much thinner and more flexible. The performance enhancement provided by the STF may be due to an increase in the yarn pullout force upon transition of the STF to its rigid state.

Acknowledgements

This work has been supported through the Army Research Laboratory CMR program (Grant No. 33-21-3144-66) through the Center for Composite Materials of the University of Delaware. The authors acknowledge the experimental assistance of Mr. Kyle Miller. Additionally, the authors are grateful to Ken Langford and Hexcel Schwebel for providing the Kevlar, and Pete Dehmer and Melissa Klusewitz for their assistance with the gas gun experiments.

References

1. P. M. CUNNIFF, *Textile Research Journal* **62** (1992) 495.
2. NIJ standard-0101.04 "Ballistic Resistance of Personal Body Armor" (2001).
3. S. BAZHENOV, *J. Mater. Sci.* **32** (1997) 4167.
4. M. J. N. JACOBS and J. L. J. VAN DINGENEN, *ibid.* **36** (2001) 3137.
5. D. I. LEE and A. S. REDER, in TAPPI Coating Conference Proceedings (1972) p. 201.
6. R. L. HOFFMAN, *J. Coll. Int. Sci.* **46** (1974) 491.
7. H. A. BARNES, *J. Rheol.* **33** (1989) 329.
8. G. BOSSIS and J. F. BRADY, *J. Chem. Phys.* **91** (1989) 1866.
9. R. S. FARR, J. R. MELROSE and R. C. BALL, *Phys. Rev.* E **55** (1997) 7203.
10. D. R. FOSS and J. F. BRADY, *J. Fluid Mech.* **407** (2000) 167.
11. A. A. CATHERALL, J. R. MELROSE and R. C. BALL, *J. Rheol.* **44** (2000) 1.
12. P. D. D'HAENE, J. MEWIS and G. G. FULLER, *J. Coll. Int. Sci.* **156** (1993) 350.
13. J. W. BENDER and N. J. WAGNER, *ibid.* **172** (1995) 171.
14. H. M. LAUN, R. BUNG, S. HESS, W. LOOSE, O. HESS, K. HAHN, E. HÄDICKE, R. HINGMANN, F. SCHMIDT and P. LINDNER, *J. Rheol.* **36** (1992) 743.
15. J. W. BENDER and N. J. WAGNER, *ibid.* **40** (1996) 899.
16. M. C. NEWSTEIN, H. WANG, N. P. BALSARA, A. A. LEFEBVRE, Y. SHNIDMAN, H. WATANABE, K. OSAKI, T. SHIKATA, H. NIWA and Y. MORISHIMA, *J. Chem. Phys.* **111** (1999) 4827.
17. B. J. MARANZANO and N. J. WAGNER, *J. Rheol.* **45** (2001) 1205.
18. B. J. MARANZANO and N. J. WAGNER, *J. Chem. Phys.* **117** (2002) 10291.
19. B. KAFFASHI, V. T. OBRIEN, M. E. MACKAY and S. M. UNDERWOOD, *J. Coll. Int. Sci.* **181** (1997) 22.
20. B. J. MARANZANO and N. J. WAGNER, *J. Chem. Phys.* **114** (2001) 10514.
21. H. M. LAUN, R. BUNG and F. SCHMIDT, *J. Rheol.* **35** (1991) 999.
22. R. HELBER, F. DONCKER and R. BUNG R, *J. Sound and Vibration* **138** (1990) 47.
23. L. DISCHLER, T. T. MOYER and J. B. HENSEN, US Patent no. 5776839 (1998).
24. R. G. LARSON, in "The Structure and Rheology of Complex Fluids" (Oxford University Press, 1999).
25. Y. S. LEE and N. J. WAGNER, *Rheol. Acta* **42** (2003) 199.
26. J. F. BRADY, *J. Chem. Phys.* **99** (1993) 567.
27. D. A. SHOCKEY, D. C. ERLICH and J. W. SIMONS, DOT/FAA/AR-99/71 (1999).

Received 17 October 2002
and accepted 9 April 2003